Improving the performances of current optical interferometers & future designs
Proceedings of Haute Provence Observatory Colloquium (23-27 September 2013)
Edited by L. Arnold, H. Le Coroller & J. Surdej

Some Astronomical Applications of High Accuracy Stellar Interferometry

B. Mennesson

Jet Propulsion Laboratory, California Institute of Technology, 4800 Oak Grove Dr, Pasadena CA 91009, USA

Abstract.
Optical astronomical interferometry has seen spectacular progress over the last two decades, notably in terms of spatial/spectral resolution, sensitivity, and in the number of accessible baselines. A significant (x 100) parallel improvement has taken place in the accuracy of interferometric measurements, whether phase or amplitude related. This evolution is important because higher measurement accuracy directly translates into higher contrast observations, which is key for a number of astronomical investigations demanding both high resolution and high contrast at the same time. This includes the characterization of molecular layers in the extended atmospheres of evolved stars, the direct imaging of surface oblateness in fast rotating stars, the direct measurement of Cepheids angular diameter changes vs pulsation - and subsequent distance determination -, the detection of faint exozodiacal dust around mature stars, and the search for sub-stellar companions to nearby stars. The latter two applications have particularly driven the field improvements over the last few years. Contrast levels of 1000:1 or better have now been achieved at several facilities, and there are prospects for an other tenfold gain in the near future, notably with the Large Binocular Telescope Interferometer (LBTI).

1. Introduction

Over the last 15-20 years, the main instrumental developments seen in optical interferometry have concentrated on improving critical capabilities: angular resolution (e.g. ten Brummelaar et al. 2005), spectral resolution (e.g. Weigelt et al. 2010), sensitivity (e.g. Woillez et al. 2013, Burtscher et al. 2013) and (u,v) plane coverage (e.g. Kloppenborg et al. 2010, Balan et al. 2010, Le Bouquin et al. 2011). In parallel to these observational efforts, and driven by a number of scientific niches, large progress has also been made in terms of interferometric contrast. The dynamic range achievable by interferometry is directly related to measurement accuracy, whether considering phase or amplitude-based observables. While "high" dynamic range (100:1 or higher) will always be benefitial, it is more or less critical depending on the astronomical application. High contrast is mandatory in some specific fields such as the detection of faint structures in the planet forming region of young and mature stars, or direct measurements of

stellar pulsation. Figure 1 sketches what kind of studies are enabled at various interferometric contrast levels, assuming adequate capabilities are available for all other observing parameters.

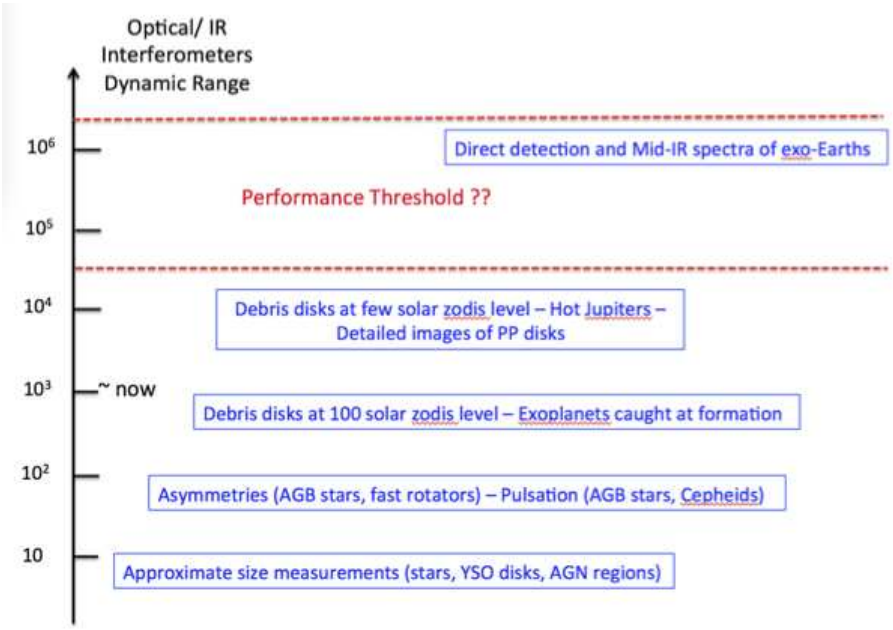

Figure 1.: *Schematic view of astronomical observations enabled by various degrees of interferometric contrast. Each application has its own minimum performance threshold. While broad-band iterferometric contrast better than* 10^6 *has already been demonstrated in the lab, the current state of the art for astronomical observations is around 1000:1.*

A major driver for the development of high accuracy interferometry has been the direct detection and characterization of exoplanets. It was first proposed for the most challenging application of all in that field: the direct detection of Earth-like extrasolar planets using mid-infrared space nulling interferometry (Bracewell 1978, Leger et al. 1996, Beichman et al. 2006). In that case, a final (post calibration) contrast of $\simeq 10^6$ is required. It has already been successfully demonstrated in the laboratory at both visible (Haguenauer & Serabyn 2006) and mid-infrared wavelengths (Martin & Booth 2010), but remains far above the current on-sky capabilites of stellar interferometers. Indeed, the best point source detection limits reached by stellar interferometry so far are a few 100:1 to $\simeq$ 1000:1, as demonstrated at the VLTI with the PIONIER beam combiner (Absil et al. 2011) and with the CHARA interferometer MIRC instrument (Zhao et al. 2011). Both instruments made use of accurate phase closure measurements in the near infrared (H-band) across 4 or more baselines, with the goal of detecting faint companions to mature stars and eventually search for exoplanets around young stars (PIONIER), or measure spectra of hot Jupiters previously detected by radial velocity studies (MIRC). This 1000:1 point source contrast is also the limit

reached by current 8m telescope aperture masking experiments conducted at Keck (NRM: Kraus & Ireland 2012, Hinkley et al. 2011) and at the VLT (NACO/SAM: Huelamo et al. 2011), which also measure interferometric phase closures from a limited number of sub-apertures. In spite of offering similar contrast performance at significantly lower angular resolution than CHARA/MIRC or VLTI/PIONIER, these single dish instruments already provided "images" of planetary candidates caught at formation around a few very young stars. The reason is that operating on large telescopes, non redundant aperture masks have a higher sensitivity, and benefit from a larger number of sub-apertures and baselines. They can also operate at more favorable infrared wavelengths, such as L or M band, where exoplanets are brighter and the required contrast is less. These results make it clear that an LMN band instrument operating at the VLTI Unit Telescopes and providing high accuracy phase closure measurement capability would be able to detect and characterize very young exoplanets around many YSOs. The next generation MATISSE instrument (Lopez et al. 2012) may have the potential for such observations, specially if more emphasis is put on phase closure accuracy over the years. Such studies might be even more compelling with some future dedicated planet formation imaging (PFI: http://planetformationimager.org/) interferometric facility, assuming it offers the required combination of sensitivity, (u,v) plane coverage and dynamic range in the near to mid-infrared.

A limit of phase closure measurements, or any interferometric observations based on phase information only, - e.g. differential phase, differential closure phase, closure phase nulling (Duvert et al. 2010) -, is that it is only sensitive to the asymmetric part of the objects brigthness distribution. In particular, it is insensitive to the main emission of circumstellar disks, and can not distinguish between a clump in a bright extended disk and a fainter isolated point source. It is clear that both visibility amplitude and phase information should be measured accurately to best constrain interferometric observations. I concentrate hereafter on the methods used to measure accurate visibility *amplitudes*. As an illustration, I present examples of astronomical objects studied at increasingly high visibility (or equivalently null) accuracy: extended molecular atmospheres around late type stars, Cepheids, warm and hot debris disks around mature stars. I then conclude by discussing new ideas, promising results and future prospects for even higher performance, specially in the context of the LBTI exo-zodi nulling survey (Hinz 2013).

2. Applications to the study of stellar atmospheres and pulsation

2.1 Fast Rotators

As visibility measurement accuracy gets down to a few percent, an interesting application in stellar physics is the observational study of gravity induced limb darkening in fast rotating stars (i.e. with surface rotational velocites greater than $\simeq$ 100 km/s). The distinctive observational signatures of rapid rotation were first described by von Zeipel (1924), beginning with the expection that centrifugal forces would distort the photospheric shape and that the resulting oblateness would induce lower effective temperatures at the equator, an effect known as gravity darkening. A good illustration of this phenomenon is Altair, a rapidly rotating hot star with a significant ($\simeq$ 14%) disk asymmetry first detected

with the Palomar Testbed Interferometer (Van Belle et al. 2001) and whose surface was later imaged in great details by multi-baseline interferometry with CHARA/MIRC (Monnier et al. 2007). MIRC images confirm the basic picture of gravity darkening induced by rapid rotation: they show Altair's photosphere to be oblate with a bright region identifiable as the stellar polar region and a dark equatorial band with approximately 60-70% of the brightness at the pole, broadly consistent with expectations for the near-infrared from previous models. Images show however a stronger darkening along the equator than would be predicted with any von Zeipel-like gravity darkening prescription assuming uniform stellar rotation, and a uniform gravity limb darkening coefficient significantly smaller than in the von Zeipel model. Such accurate imaging studies of gravity darkening have now been carried at NPOI and CHARA on a number of other fast rotators, among which Vega (Aufdenberg et al. 2006), Achernar (Domiciano de Souza), Regulus (McAlister et al. 2005), and Alderamin (Van Belle et al. 2006). Both differential rotation and/or gravity darkening laws versus latitude could explain the observations of Altair and the few other fast rotators observed. Whatever the explanation, these interferometric observations convincingly establish the case for stellar physics beyond the standard models used today to describe fast rotating stars.

2.2 Extended molecular layers around late type stars

Historically, the first instrument to provide high visibility accuracy (of the order of 1% or better, Perrin et al. 1998, Merand et al. 2005) was the IOTA/FLUOR instrument (Coude du Foresto 1998), which used single-mode waveguides for optical recombination and calibration of atmospheric effects. As these accurate visibility measurements became available, a number of new results were quickly obtained on evolved stars, illustrating the impact of a ten fold gain in visibility accuracy. The effective temperature scale of giants was extended to types later than M6 (Perrin et al. 1998), the photospheric pulsation of R Leonis was detected in the near infrared for the first time (Perrin et al. 1999) and there was now clear evidence for very extended molecular layers (H_2O, CO, etc) around O-rich Miras and semi-regular variables (Mennesson et al. 2002, Perrin et al. 2004), confirming what was suspected from high resolution spectroscopic observations. The latter discovery, and in particular the results of narrow filter measurements, allowed to reconcile a variety of discrepant "diameter" estimates coming from interferometric observations at different wavelengths and spatial resolutions. High visibility accuracy was key to distinguishing the effect of molecular species variable absorption versus time and wavelength, appearing at mid-spatial frequencies, from that of stellar pulsation, occuring at higher spatial frequencies characteristic of the photosphere. In particular, when taking the contribution of upper molecular layers properly into account, Mira's photospheric radii were found significantly smaller than previously measured, which could favor a fundamental mode of pulsation (Wood 1990). While these now fairly archaic IOTA observations naturally lacked sensitivity and spectral resolution with 40 cm siderostats, they paved the way to next generation fiber based /integrated optics instruments used on larger more sensitive telescope arrays, such as CHARA/MIRC and VLTI PIONIER. As for FLUOR, it is still on the sky in a rejuvenated form. It was moved to the CHARA array in 2005 and was recently upgraded with new optics and acquisition software (Scott 2013, Mennesson 2013).

2.3 Cepheids pulsation and circumstellar material

Another application that relies on accurate visibility measurements is the determination of accurate distances to Cepheids, the goal there being to calibrate the Cepheids period - absolute luminosity relation used for the determination of local and cosmological distances, which play themselves a critical role in the determination of the Hubble constant (e.g Sandage et al. 2006). Stellar interferometry allows to directly measure distances to pulsating stars by the way of the parallax pulsation technique, also known as the Baade- Wesselink method (Baade 1926, Wesselink 1946), which compares the actual change in angular diameter and the change in pulsation velocity V_{rad} in order to measure distances. A limitation in using this method however, is that spectroscopy does not directly measures the pulsation velocity, but the projected velocity $V_p = p.V_{rad}$, integrated over the surface on the star, where p is the so-called "projection factor". A first contribution of stellar interferometry has then been to determine this projection factor with a better precision that previously available, applying the Baade Wesselik equation to δ Cep, the only Cepheid with a well known physical distance, and for which accurate angular diameter measurements were obtained from CHARA (Merand et al. 2005). The p factor value was pinned down to 1.27 ± 0.04, while theoretical model predicted values between 1.27 (Nardetto et al. 2004) and 1.45 (Sabbey et al. 1995). A second major contribution of interferometry has been the realization that many Cepheids are surrounded by large envelopes many stellar diameters in size (Kervella et al. 2006, Galenne et al. 2013b) emitting a few percent of the total near infrared flux, and whose characteristics need to be properly taken into account in order to use the Baade-Wesselink method. Finally, recognizing the modeling uncertainties related to these newly discovered complex circumstellar structures around Cepheids, an other powerful approach to the problem of estimating Cepheid distances is the observation of Cepheids in binary systems. This has been the object of recent high accuracy interferometric observations (Galenne et al. 2013a and 2014) providing direct detection of faint stellar companions, accurate measurements of orbital periods, dynamical masses and angular separations, while Kepler's third law provides the physical separation necessary to derive stellar distances.

3. Exozodiacal disks

The outer colder parts of debris disks, analogous to our solar system Kuiper belt, were first detected via their mid infrared or far infrared excess emission, and then abundantly imaged at visible to sub-millimeter wavelengths. Conversely, very little is known about the hotter (> 200K) dust component of debris disks, concentrating in the inner few AUs of the stellar environment where rocky planets may have formed, similar to the zodiacal dust found in the inner solar system. Indeed, only a few hot debris disks have been found by Spitzer around mature stars via excess emission at wavelengths of 24 microns or shorter (Su et al. 2006, Wyatt et al. 2007, Lawler et al. 2009, Bryden et al. 2009), and very few have been unambiguously resolved from the ground at mid-infrared wavelengths (e.g. Smith et al. 2009, Stock et al. 2011, Millan-Gabet et al. 2011). This observational difficulty results from several factors: the exozodiacal disks small sizes and their faintness relative to the host stars. Indeed, while cold debris disks cause very

significant excesses readily detectable at far infrared wavelengths, exozodiacal material located in the inner few AU only contributes a small fraction of the stellar flux. In order to reliably detect such tiny ($\simeq$ 1% or less) excess emission over that expected from the photosphere, direct imaging is required, with the ability to spatially resolve dust from the central star. In the visible, where dust is essentially seen through starlight scattering, the contrast required is extremely high and only a space or balloon borne coronagraph can provide adequate performance. In the infrared, exozodi disks produce significant thermal emission and contribute a larger fraction of the stellar flux, making it the spectral range of choice for ground-based exozodi studies. With the combination of contrast and spatial scales at play, typically 0.1 to a few AU, such direct infrared observations are best accomplished using high accuracy long baseline interferometry. This was the main goal of the Keck Interferometer Nuller (KIN), a long baseline (85m) high contrast instrument operating between 8 and 13 microns, specially built to spatially resolve faint structures next to bright stars (Colavita et al. 2013, Serabyn et al. 2012, Mennesson et al. 2003). Exozodi observations were carried out with the KIN between 2008 and 2011 through three different Key Science programs (respectively led by Eugene Serabyn, Phil Hinz and Marc Kuchner) and one PI program (led by Mennesson). It targeted 47 nearby main sequence stars overall, 40 of which had no companion known within the interferometric field of view ($\simeq$ 0.5" at FWHM). These KIN observations have just been fully reduced (Mennesson et al. in preparation) and we summarize hereafter some of the key conclusions. These are based on the 8 to 9 microns data alone, which provide the highest signal to noise measurements, with final null accuracies (1 σ) ranging from of 0.1% to 0.5%, depending on the 10 microns stellar flux. We found only one star with a large excess imputable to dust emission (η Crv), while four more stars showed a significant ($> 3\sigma$) excess: β Leo, β UMa, ζ Lep and γ Oph. Overall, KIN excesses were detected more frequently around A-type stars than later types, and around stars already suspected to have cold dust around them through far infrared excesses, suggesting some dynamical link between the inner (zodi-like) and outer (Kuiper belt like) dust populations. A fairly surprising result is that no significant mid-infrared excess is generally found around sources with a previously reported $\simeq$ 1% near-infrared resolved excess. If dust emission is really at stake in these near-infrared detections (Absil et al. 2013), the absence of a strong mid-infrared counterpart would point to populations of very hot and small (sub-micronic) grains piling up close to the sublimation radius. Since such grains should be rapidly expelled from the inner system by radiation pressure, this would indicate some inordinate replenishment rates or yet poorly understood dynamical effects trapping or maintaining dust close to the sublimation radius. A statistical analysis of the overall measurements also suggests that many of the sample stars have excesses close to the KIN detection limit of a few 100 zodis, and hence constitute prime candidates for more sensitive exo-zodi surveys such as the one just starting with the Large Binocular Telescope Interferometer (LBTI, see section 4.1).

4. Future prospects in high contrast interferometry

What is the future of high contrast astronomical interferometry and how do we get there? As the interferometric detection of very faint point sources and espe-

cially young and/or hot exoplanets is concerned, there are prospects for reducing current systematics. As explained in section 1, the contrast provided by ground based phase closure measurements is currently limited to 1000:1 or so. This limit is common to long baseline interferometric observations and aperture masking measurements on large telescopes, When dealing with systematics at such low levels, all temporal and spatial effects have to be properly understood and minimized, including the effects of finite integration over spatial, temporal and wavelength domains. Such effects and mitigation strategies have been studied recently by Mike Ireland (2013), who concluded that temporal phase noise and photon noise limited detections should be accessible. Some new ideas have also been proposed to combine nulling with phase closure in order to access deeper point source contrasts than with any of the two techniques used individually.

While exoplanets direct detection will likely continue to drive future improvements in terms of phase closure and differential phase accuracy for high contrast interferometric measurements, we concentrate hereafter on the immediate problem of measuring visibility amplitudes at the $\simeq 10^{-4}$ accuracy level, as required by the LBTI exo-zodi survey. We also discuss a fairly new observing/ data analysis technique which already demonstrated near infrared visibility measurements down to an absolute accuracy of 0.1% or better (Mennesson et al. 2011a & b), and assess its applicability to the LBTI contrast challenge in the mid-infrared.

4.1 LBTI Exozodi survey

The Hunt for Observable Signatures of Terrestrial planetary Systems (HOSTS) on the Large Binocular Telescope Interferometer (LBTI) will survey nearby stars for faint exozodiacal dust (exozodi). LBTI-HOSTS (Hinz et al. 2013) should be the first survey capable of measuring exozodi at the 10 zodi level, which corresponds to a null measurement accuracy of $\simeq 10^{-4}$, ten times better than the best results achieved by the KIN survey. Exozodi of this brightness would still be the major source of astrophysical noise for a future space telescope aimed at direct imaging and spectroscopy of habitable zone terrestrial planets. Detections of such warm dust will also reveal new information about planetary system architectures and evolution. The HOSTS survey target list is currently being defined by the LBTI science team (Weinberger et al. 2014) and will reflect both objectives. The space mission-driven approach concentrates on F, G, and K-type stars that are the best targets for future direct observations of exoEarths, thereby providing model-independent ground truth dust observations. However, not every potential target of a future exoEarth mission can be observed with LBTI, and a complementary approach selects targets based only on what exozodi sensitivity could be achieved, without consideration of exoEarth mission constraints. This naturally selects more luminous stars (A and early F-type stars). In both cases, all stars are close enough to Earth that their habitable zones are resolvable by LBTI and bright enough at N-band (10 μm) to provide excellent sensitivity. Clearly, the LBTI requirement to measure astronomical nulls (or visibilities) down to a relative accuracy level of 10^{-4} is a daunting one, specially in the mid-infrared, where warm optics thermal emission is extremely high. There are however several reasons why the LBTI may provide more accurate results that the KIN survey:

- Lower thermal background. With its adaptive secondary mirrors, the LBTI only has 3 warm optics before the cold beam combiner, and the expected total warm train emissivity is 10 to 15%, to be compared to $\simeq 95\%$ at KI. The

total number of optics is also less than at KI and the recombination strategy uses a single beam splitter, making the overall instrument transmisison higher than at KI. Overall, the photometric signal to noise is expected to be about ten times higher at any given mid-infrared wavelength, which also opens the door to operation at 10 - 12 microns (rather than 8-9 microns, optimum for sensitivity at Keck), a wavelength range where wavefront correction is better and where the dust over star flux contrast is likely more favorable. Background estimation still remains a difficult task at LBTI: even with the warm optical train low emissivity, background counts are comparable to Vega's flux at 11 microns. In order to measure a 10^{-4} null on a 1 Jy star, the thermal background must hence be estimated with no systematic bias down to a few ppm.

- Accurate background estimation. While the KIN used a complex 4-beam phase modulation scheme to reject the large background signal and its slow fluctuations (Serabyn et al. 2012), the LBTI uses simultaneous background measurements in focal plane areas close to the science image. Regular nods of the telescopes are then used to regularly measure the background offset between the 2 regions of the detector. Using nods every 90 seconds and 40 mn of observations, LBTI sky tests have already demonstrated mean background estimation down to a level of 2ppm between 10 and 12 μm and spectrally white measurement error down to the background photon noise level (Defrere and Mennesson, in preparation).

- No longitudinal dispersion. Because of the common binocular mount used for the observations, the interferometric baseline is always perpendicular to the line of sight and there are no differential longitudinal dispersion or differential atmospheric refraction effects between the 2 beams.

- Smaller baseline. With a 14.4 m center to center baseline, LBTI observations are less sensitive to calibrator diameter uncertainties than the KIN observations. Since the uncertainty on the null goes as the square of the projected baseline, the impact of calibrator diameter uncertainties is reduced by a factor of 30 to 40. Using a smaller baseline and a common mount also significantly reduces the complexity inherent to beam transport and long delay lines.

- A series of two-beam nulling observations conducted in the near infrared at the Palomar Hale Telescope have recently demonstrated the ability to measure astrophysical nulls at a level of a few 10^{-4} at 1σ. Moreover, this accuracy could be achieved while the observed mean null levels and temporal fluctuations were 100 higher or more. These Palomar results used the "Null Self Calibration" method (Mennesson et al. 2011b, Hanot et al. 2011), which should be applicable to the LBTI mid-infrared observations, at least to some extent, as explained in the next section.

4.2 Null Self Calibration (NSC) method

The NSC method is based on the analysis of the probability distribution of the interferometric signal measured while stabilizing the optical path difference (OPD) around the central dark fringe, i.e. the deepest white light null (Mennesson et al.

2011a, Mennesson et al. 2013). It was first demonstrated with the Palomar Fiber Nuller (PFN), a mini near-infrared (broad K-band) nulling interferometer developed at JPL since 2006 (e.g. Mennesson et al. 2006, Martin et al. 2008), which uses two (3 x 1.5m) sub-aperture beams of the primary mirror located 3.2m apart and recombines them coherently into a common single-mode fiber. The PFN is a visitor instrument installed in the Palomar 200 inch Cassegrain cage and located downstream of the AO system which stabilizes the 2 beams OPD down to $\simeq$ 200 nm rms at K band. Figure 2 shows as an illustration the results obtained on the bright star α Boo, for which consecutive NSC based astrophysical null depth estimates were derived over one hour of observation and remained stable at the few 10^{-4} level. Note that for the PFN, we computed the observed distribution of the instantaneous null level (interferometric signal normalized by constructive interference signal). Interestingly, and as shown in the upper two panels, the observing conditions (relative beam intensity, average phase difference and phase jitter) and resulting null level distributions can vary a lot with time, yielding very different average null levels: 0.065 and 0.095 in that case. However, the astronomical null values derived from the NSC fitting method are significantly lower, and much closer to each other: 0.0130 ± 0.0005 and 0.0132 ± 0.0006. The advantages of the NSC method is that it uses the whole data distribution (not just its average or some other ensemble characteristics) to make an estimate of the astronomical null or visibility, and that it takes out the coherence loss effects due to opd jitter (piston) and intensity mismatch. The final calibrated visibility estimate derived for α Boo was V= 0.9739 ± 0.0006 (astronomical null = 0.0132 ± 0.0003), fully consistent with the value expected from its near infrared diameter measured at much longer baselines. Astrophysical nulls at the 10^{-3} level or lower have since been measured on smaller fainter targets, also with accuracies of a few 10^{-4} (Mennesson et al. 2011a and subsequent unpublished results).

However, for the NSC method to be effective, four main requirements must be met (e.g. Mennesson et al. 2013): (1) the beams shall eventually be recombined in a common single-mode waveguide, (2) the optical path difference must be stabilized around the central dark fringe with no fringe hop (i.e. $\simeq \lambda/5$ rms jitter is enough), (3) the interferometric signal must be sampled significantly faster than the atmospheric coherence time (or fringe tracker closed loop bandwidth), (4) background and individual beam signals must be recorded close in time to the fringe data. Near infrared feed-forward fringe tracking has recently been demonstrated at the LBTI (Defrere et al. in preparation), providing adequate levels of mid-infrared OPD stabilization (point 2). The LBTI nulling instrument observational procedure has also been designed to meet requirements (3) & (4). In particular, and as stated above, instantaneous background estimation errors are well approximated by zero mean gaussian white noise, and no significant long term bias was found in the background estimates, down to the few ppm level. This means that the mid-infrared background noise behavior will be no different from detector shot noise errors, which are dominating in the case of near infrared PFN observations. The only NSC requirement that is not met by the LBTI nuller is that the instrument is not strictly "single-mode", i.e. that the null observed is not just a function of beam relative intensities and relative piston. Higher order of differential phase aberrations will be present in the measured nulls, because the two telescope beams are not recombined in a common single-mode waveguide (point 1). However, we hope to mitigate such high spatial order effects by only using the central part of the PSF for all null and photometric computations. With

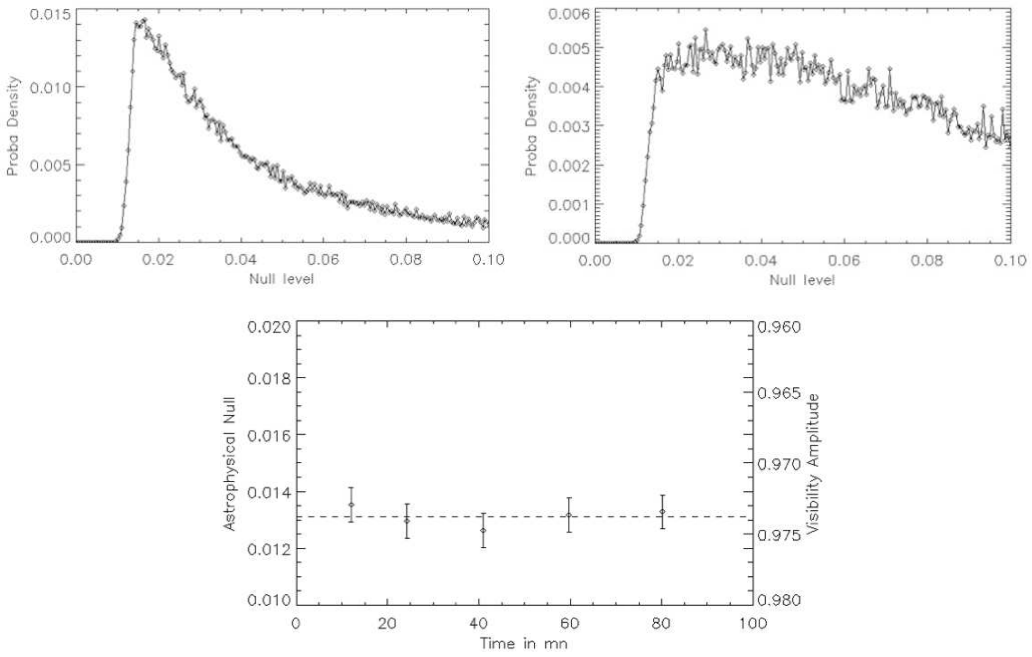

Figure 2.: *Palomar Fiber Nuller measurements of α Boo. Top panels: observed distributions of instantaneous interferometric signals (normalized to constructive interference case to provide an instantaneous null level) recorded at two different times - second and fifth measurements displayed in lower panel-. Lower panel: Object's visibility -right vertical axis- and equivalent astrophysical null depth -left vertical axis- measured as a function of time. No calibrator star was used; visibilities are derived using the null (or visibility) histogram modeling NSC technique (Mennesson et al. 2011a & 2011b, Hanot et al. 2011). All individual visibility error bars are about 0.0006. The final calibrated visibility estimate is V= 0.9739 +/- 0.0006. The dashed line indicates the astronomical null (or visibility) expected at the same spatial frequency, using α Boo's limb darkened diameter measured independently by NIR long baseline interferometry (Perrin et al. 1998, Lacour et al. 2008). A similar data reduction method will be applied to the mid-infrared LBTI nulling survey data.*

mid-infrared Strehl ratios higher than 98% and higher order wavefront errors leaking most light outside of that central diffraction limited area, we expect a small impact on the observed null distribution and the the NSC fitting procedure results.

5. Conclusions

High contrast interferometry is coming of age, with a number of facilities having already demonstrated point source detection capabilities approaching 1000:1 at angular scales of just a few milliarcseconds. This is already a remarkable performance given that the multi-baseline imaging systems providing these results are first generation multi-beam combiners, not necessarily optimized for high accuracy phase closure measurements. With some return of experience and the lessons learnt from aperture masking on single telescopes, high contrast long baseline stellar interferometry should be able to access dynamic ranges of 10^4:1 or so on point sources in the next decade. However, this will only happen if a dedicated effort is pursued in that direction. This could take place at VLTI and CHARA in particular, since they are currently at the forefront of such programs -, or at future interferometric facilities such as the Planet Formation Imager which will likely have ambitious goals in terms of contrast. As the detection of extended sources is concerned, such as circumstellar material around pulsating stars and faint exo-zodi structures around mature stars, high visibility amplitude measurement accuracy is required. In particular, the exo-zodi nulling surveys led in the mid-infrared at the Keck Interferometer and in the near infrared at CHARA (Absil 2013) have already demonstrated contrast limits of 500:1 or more. With its requirement of reaching interferometric contrasts of 10^4 or so, there is no doubt that the LBTI will stretch nulling (or equivalently visibility) measurement accuracy to its limits for the years to come. In the same way that long baseline phase closure experiments can benefit from aperture masking techniques developed for single telescopes, the LBTI will capitalize on new nulling data reduction techniques elaborated at the Palomar Hale telescope for the Fiber Nuller instrument. Using near infrared nulling on a short 3.2m baseline and the "Null Self Calibration" data reduction method (also applicable to visibilities), the Palomar Fiber Nuller demonstrated null accuracies down to a few 10^{-4}. These null levels are the deepest reported so far on the sky, and are commensurate with the ambitious LBTI objectives.

Acknowledgements. This work was performed at the Jet Propulsion Laboratory, California Institute of Technology, under contract with NASA. The Keck Observatory was made possible through the generous financial support of the W.M. Keck Foundation.

References

Absil, O., 2011, A&A, 535, 68
Aufdenberg, J.M. et al. 2006, ApJ, 465, 664
Baade, W. 1926, Astronomie Nachrichten, 228, 359
Balan, A. et al. 2010, AJ, 139, 2269

Beichman, C. et al. 2006, SPIE, 6268, 25
Bracewell, R. N., 1978, Nature, 274, 780
Bryden, G. et al. 2009, ApJ, 785, 89
Burtscher, L. et al. 2013, A&A, 558, 149
Colavita, M.M. et al. 2013, PASP, 125, 1226
Coude du Foresto, V. et al. 1998, Proc. SPIE Vol. 3350, p. 856-863, Astronomical Interferometry, Robert D. Reasenberg
Domicinao de Souza, A. et al. 2003, A&A, 407, L47
Duvert, G. et al. 2010, A&A, 509, 66
Galenne, A. et al. 2014, A&A, 561, 3
Galenne, A. et al. 2013b, A&A, 558, 140
Galenne, A. et al. 2013a, A&A, 552, 21
Haguenauer, P. & Serabyn, E. 2006, Applied Optics, 45, 12
Hanot, C., et al. 2011, ApJ 729, 110
Hinkley, S. et al. 2011, ApJ, 730, L21
Hinz, P. 2013, AAS Meeting 221
Huelamo et al. 2011, A&A, 528, 7
Ireland, M. 2013, MNRAS, 433, 1718
Kraus, A. & Ireland, M. 2012, ApJ, 745, 5
Kervella, P. et al. 2006, A&A, 448, 623
Kloppenborg, B. K., et al, 2010, Nature, 464, 870
Lacour, S. et al. 2008, A&A, 485, 561
Lawler, S.M. et al. 2009, ApJ, 705, 89
Le Bouquin, J. B., et al. 2011, A&A, 535, 67
Leger, A. et al. 1996, Icarus, 123, 249
Lopez, B. et al. 2012, Proc. of the SPIE , Vol. 8445
Martin, S. R. & Booth, A. J., 2010, 511, L1
Martin, S. R. et al, 2008, Proc. of the SPIE, Vol. 7013. Edited by Schller, Markus; Danchi, William C.; Delplancke, Franoise.
McAlister, H. A., 2005 et al., 2005, ApJ 628, 439
Mennesson, B. et al. 2013, Journal of Astronomical Instrumentation, Vol. 2, Special Issue Optical and Infrared Interferometry; Guest Editors: Theo ten Brummelaar, Peter Tuthill and Gerald van Belle
Mennesson, B. et al. 2011a, ApJ, 736, 14
Mennesson, B. et al. 2011b, ApJ 743, 178
Mennesson, B. et al. 2006, in SPIE Conf. Ser. 6268, Advances in Stellar Interferometry, ed. J.D. Monnier, M. Scholler, W.C. Danchi, 95
Mennesson, B. et al. 2003, Conference on Towards Other Earths: DARWIN/TPF and the Search for Extrasolar Terrestrial Planets, Edited by M. Fridlund, T. Henning, ESA SP-539, p. 525 - 528
Mennesson, B. et al. 2002, ApJ, 579, 446
Merand, A. et al. 2005, A&A, 438, L9

Merand, A. et al. 2006, in SPIE Conf. Ser. 6268, Advances in Stellar Interferometry, ed. J.D. Monnier, M. Scholler, W.C. Danchi, 46

Millan-Gabet, R. et al. 2011, ApJ, 734, 67

Monnier, J. et al. 2007, Science, 317, 342

Nardetto, N. et al. 2004, A&A, 428, 131

Perrin, G. et al., 2004, A&A, 426, 279

Perrin, G. et al., 1999, A&A, 345, 221

Perrin, G. et al., 1998, A&A, 331, 619

Sabbey C.N. et al. 1995, ApJ, 446, 250

Sandage, A. et al. 2006, ApJ, 653, 843

Scott, N. et al. 2013, Journal of Astronomical Instrumentation, Vol. 2, Special Issue Optical and Infrared Interferometry; Guest Editors: Theo ten Brummelaar, Peter Tuthill and Gerald van Belle

Serabyn, E. 2012, ApJ, 748, 55

Smith, R., Wyatt, M.C. & Haniff, C.A. 2009, A&A503, 265

Stock, N. et al. 2010, ApJ, 724, 1238

Su, K. Y. L. et al. 2006, ApJ, 653, 675

ten Brummelaar, T. A. et al. 2005, ApJ, 628, 453

van Belle G. T. , et al., 2006, ApJ 637, 494

van Belle G. T., et al. 2001, ApJ 559, 1155

Von Zeipel, H. 1924, MNRAS 84, 684

Weigelt, G. et al. 2011, A&A, 527, 103

Weinberger, A. 2014, AAS Meeting 223

Wesselink, A. J., et al., 1946, Bulletin of the Astronomical Institutes of the Netherlands, Vol. 10, p.91

Woillez, J. et al. 2013, in Optical and Infrared Interferometry III. Proceedings of the SPIE, Volume 8445

Wood, P. R. 1990, in From Miras to Planetary Nebulae, ed. M. O. Mennessier & A. Omont (Gif-sur-Yvette: Editions Frontieres), 67

Wyatt, M. et al. 2007, ApJ, 658, 569

Zhao, M., et al. 2011, PASP, 123, 964